Available online at www.sciencedirect.com
SCIENCE DIRECT®
International Journal of Heat and Fluid Flow 24 (2003) 137–144
International Journal of HEAT AND FLUID FLOW
www.elsevier.com/locate/ijhff

# Analytical solution for dynamic pressurization of viscoelastic fluids

S.H. Hashemabadi [a], S.Gh. Etemad [b], J. Thibault [c,*], M.R. Golkar Naranji [a]

[a] Department of Chemical Engineering, Amir Kabir University, Tehran, Iran
[b] Department of Chemical Engineering, Isfahan University of Technology, PO Box 84155-133, Isfahan, Iran
[c] Department of Chemical Engineering, University of Ottawa, Colonel By Hall, Ottawa, ON, Canada KIN 6N5

Received 9 April 2002; accepted 7 August 2002

**Abstract**

The flow of simplified Phan-Thien–Tanner model fluid between parallel plates is studied analytically for the case where the upper plate moves at constant velocity. Two forms of the stress coefficient, linear and exponential, are used in the constitutive equation. For the linear stress coefficient, the dimensionless pressure gradient, the velocity profile and the product of friction factor and Reynolds number are obtained for a wide range of flow rate, Deborah number and elongational parameter. The results indicate the strong effects of the viscoelastic parameter on the velocity profile, the extremum of the velocity, and the friction factor. A correlation for the maximum pressure rise in single screw extruders is proposed. For the exponential stress coefficient, only velocity profiles were obtained and compared with velocity profiles obtained with the linear stress coefficient.


## 1. Introduction

The pressurization technique is widely used in material processing. The purpose of pressurization is to generate pressure to force the viscous fluid to flow downstream. Pressurization can be achieved by a moving external surface parallel to the desired flow direction of the fluid with different end-point flow restrictions, a technique that is known as viscous dynamic pressurization. Single screw extrusion, calendaring and hot rolling are practical examples of this method.

Due to their simplicity and originality, parallel plates are often used to simulate the actual flow domain conditions in a single screw extruder. Because a narrow gap exists between the barrel and the screw of the extruder, assuming the fluid is flowing between parallel plates, leads to meaningful and accurate results. Tadmor and Gogos (1979) published an extensive compilation of the available information and mathematical explanation for single screw extrusion.

Materials such as polymeric fluids and foods are processed in single screw extruders, and mostly show viscoelastic behavior. One of the non-linear viscoelastic constitutive equations is the Phan-Thien–Tanner (PTT) model (Phan-Thien and Tanner, 1977; Phan-Thien, 1978), which has been derived from the network theory, and has been found to be more realistic for polymer melts and concentrated solutions in comparison with other models. One of the advantages of the PTT model over most of the other models seems to be the elongational parameter $\varepsilon$.

Bird et al. (1978) and Tanner (2000) published excellent books on engineering rheology and various viscoelastic constitutive equations. Gopalakrishna and Jaluria (1992) solved numerically the governing equation for single screw extruders with the assumption of power law model for non-Newtonian fluids. Alves et al. (2001) derived an analytical solution for the steady state channel and pipe flows with stationary walls. They used the full PTT constitutive equation with a linear stress coefficient without solvent viscosity. Davaa et al. (2001) used numerical methods to solve the fully developed laminar heat transfer for modified power law fluids flowing between parallel plates with one of the plates in motion. Oliveira and Pinho (1999) and Pinho and Oliveira (2000) derived a series of analytical solutions for the simplified Phan-Thien–Tanner (SPTT) model in duct flows and heat transfer.

The solution of viscous dynamic pressurization for a simplified PTT model fluid moving between parallel

* Corresponding author. Tel.: +1-613-562-5772; fax: +1-613-562-5172.
*E-mail address:* thibault@genie.uottawa.ca (J. Thibault).

0142-727X/02/$ - see front matter © 2002 Elsevier Science Inc. All rights reserved.
PII: S0142-727X(02)00204-7

**Nomenclature**

| | |
|---|---|
| $A$ | minimum location in $f\,Re$ graph |
| $D$ | hydraulic diameter |
| $De$ | Deborah number $\left(\frac{\lambda V}{H}\right)$ |
| $f$ | Fanning friction factor |
| $H$ | gap between parallel plates |
| $G$ | dimensionless pressure gradient |
| $Re$ | Reynolds number $\left(\frac{\rho \bar{u} D}{\eta}\right)$ |
| $p$ | pressure |
| $V$ | velocity of the moving plate |
| $u$ | velocity profile |
| $x$ | axial coordinate |
| $y$ | lateral coordinate |
| $Z$ | stress coefficient function |

*Greeks*

| | |
|---|---|
| $\alpha$ | defined by Eq. (19) |
| $\varepsilon$ | extensional parameter of the PTT model |
| $\eta$ | viscosity coefficient of the PTT model |
| $\dot{\gamma}$ | shear rate |
| $\kappa$ | location of the extremum in the velocity profile |
| $\lambda$ | relaxation time in the PTT model |
| $\xi$ | slip parameter of the PTT model |
| $\tau$ | stress tensor |

*Subscripts*

| | |
|---|---|
| 0 | value of variable at $y = 0$ (stationary plate) |
| ave | average value |
| e | exponential solution |
| l | linear solution |
| max | maximum value |
| w | at the wall |

*Superscripts*

| | |
|---|---|
| $*$ | refers to dimensionless quantities |
| – | refers to average values |

plates with one of the plates in motion has not yet been reported. The objective of the present investigation is to solve analytically the momentum governing equation for such a system that corresponds to the situation of single screw extruders. The analytical solution derived in this investigation can be used as a benchmark to validate numerical results and is more convenient to describe some specific fluid behaviors.

## 2. Problem statement

The problem considered in this investigation is depicted in Fig. 1. The geometry consists of two parallel plates that are infinite in the $x$-direction and wide enough in the $z$-direction to have negligible side effects. It is assumed that the entrance and exit conditions have a negligible effect on the flow behavior of the fluid. The valve or the die located at the discharge end of the extruder controls the flow rate of the fluid and, as a result, set the pressure inside the extruder. Therefore for most of the section of the extruder, a fully developed flow is assumed to occur.

The flow is assumed to be laminar, steady state, isothermal and incompressible. The no-slip condition exits

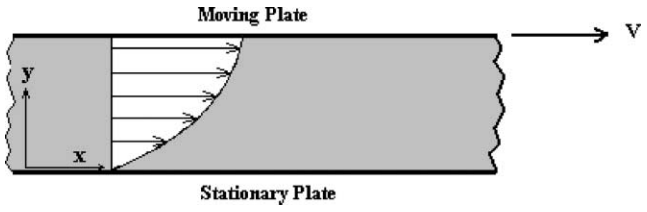


Fig. 1. Schematic diagram of the flow domain.

at the walls and the gravitational forces for the flow domain are negligible. For the situation described above, the momentum equations are

$$\frac{\partial p}{\partial x} = -\frac{\partial \tau_{yx}}{\partial y} \tag{1}$$

$$\frac{\partial p}{\partial y} = 0 \tag{2}$$

The PTT constitutive equation is given by the following equation (Bird et al., 1978):

$$Z(\mathrm{tr}\,\tau)\tau + \lambda\tau_{(1)} + \frac{\xi}{2}\lambda(\dot{\gamma}\cdot\tau + \tau\cdot\dot{\gamma}) = -\eta\dot{\gamma} \tag{3}$$

Two suggested empirical forms of $Z$ are as follows:

$$Z(\mathrm{tr}\,\tau) = \exp\left(-\frac{\varepsilon\lambda\,\mathrm{tr}\,\tau}{\eta}\right) \tag{4}$$

$$Z(\mathrm{tr}\,\tau) = 1 - \varepsilon\lambda\frac{\mathrm{tr}\,\tau}{\eta} \tag{5}$$

where $\varepsilon$ is related to the elongational behavior, $\eta$ is the viscosity coefficient of the model, $\lambda$ is the relaxation time and $\mathrm{tr}\,\tau$ is the trace of the stress tensor $\tau\cdot\xi$ is a constant parameter of the PTT model. It is related to the slip velocity between the continuum medium and the molecular network, and in this investigation it was equal to zero, which is valid for affine motion (Bird et al., 1978). $\tau_{(1)}$ is the convected time derivative of the stress and is defined by

$$\tau_{(1)} = \frac{\mathrm{D}\tau}{\mathrm{D}t} - \{(\nabla u)^{\mathrm{T}}\cdot\tau + \tau\cdot(\nabla u)\} \tag{6}$$

For the fully developed flow condition, where the velocity and stress depend only on the lateral coordinate $y$, the constitutive Eq. (3) reduces to

$$Z\tau_{xx} - 2\lambda\dot{\gamma}_{yx}\tau_{yx} = 0 \tag{7}$$

$$Z\tau_{yy} = 0 \tag{8}$$

$$Z\tau_{yx} - \lambda\dot{\gamma}_{yx}\tau_{yy} = -\eta\dot{\gamma}_{yx} \tag{9}$$

Eq. (8) indicates $\tau_{yy} = 0$, hence the trace of the stress tensor will be equal to $\tau_{xx}$. The left hand side of Eq. (1) is a function of $x$ whereas the right hand side is a function of $y$, which implies that both sides of the equation are equal to a constant value. Therefore, the pressure gradient is constant.

The shear stress ($\tau_{yx}$) can be obtained by integrating Eq. (1):

$$\tau_{yx} = \tau_0 - \left(\frac{\mathrm{d}p}{\mathrm{d}x}\right)y \tag{10}$$

$\tau_{yx}$ is a linear function of $y$ and, as a specific case, is constant in the absence of pressure gradient. $\tau_0$ is the shear stress at the stationary plate. From Eqs. (7)–(10), the normal stress $\tau_{xx}$ is obtained:

$$\tau_{xx} = -\frac{2\lambda}{\eta}\left(\tau_0 - \left(\frac{\mathrm{d}p}{\mathrm{d}x}\right)y\right)^2 \tag{11}$$

The first normal stress difference is equal to $\tau_{xx}$ while the second normal stress difference is zero. Substituting Eq. (10) into Eq. (9) gives the following equation:

$$\dot{\gamma}_{yx} = \frac{\mathrm{d}u}{\mathrm{d}y} = -\frac{Z(\mathrm{tr}\,\tau)}{\eta}\left(\tau_0 - \frac{\mathrm{d}p}{\mathrm{d}x}y\right) \tag{12}$$

As mentioned previously, two forms of $Z(\mathrm{tr}\,\tau)$ have been extensively used. The linear form is applicable when the exponential argument in Eq. (4) is small. Weak flows possess a small molecular deformation (Tanner, 2000). Therefore, the linear form of $Z(\mathrm{tr}\,\tau)$ can be employed. The shear rate ($\dot{\gamma}^*$) with the linear form of the stress coefficient is non-dimensionalized with respect to the following characteristic parameters:

$$u^* = \frac{u}{V}, \quad y^* = \frac{y}{H}, \quad x^* = \frac{x}{H}, \quad De = \frac{\lambda V}{H}$$
$$G = \frac{H^2}{\eta V}\left(\frac{\mathrm{d}p}{\mathrm{d}x}\right), \quad \tau^* = \frac{\tau H}{\eta V} \tag{13}$$

$$\dot{\gamma}^*_{yx} = \frac{\mathrm{d}u^*}{\mathrm{d}y^*} = (1 + 2\varepsilon De^2(Gy^* - \tau^*_{0l})^2)(Gy^* - \tau^*_{0l}) \tag{14}$$

where the dimensionless group $De$ is the Deborah number that is related to the level of elasticity of the fluid. The term $\varepsilon De^2$ is referred to as the viscoelastic dimensionless group. $G$ is a dimensionless group for pressure drop. For Newtonian fluid, the ratio of the pure drag flow rate to the pure pressure flow rate is equal to $6/G$. The pure drag flow rate corresponds to the situation when the axial pressure gradient is zero ($\mathrm{d}p/\mathrm{d}x = 0$), while the pure pressure flow rate applies for stationary parallel plates (Tadmor and Gogos, 1979). $\tau^*_{0l}$ is the dimensionless shear stress at the stationary plate, when the linear function of stress coefficient is used.

The boundary conditions for this situation are

$$y^* = 0 \quad u^* = 0 \tag{15}$$

$$y^* = 1 \quad u^* = 1 \tag{16}$$

### 2.1. Analytical solution, results and discussion

By integrating Eq. (14) with boundary condition (15), the dimensionless velocity profile is obtained:

$$u^* = \tfrac{1}{2}y^*(Gy^* - 2\tau^*_{0l}) + \tfrac{1}{4}\varepsilon De^2 y^*(Gy^* - 2\tau^*_{0l}) \times \left[(Gy^*)^2 + (Gy^* - 2\tau^*_{0l})^2\right] \tag{17}$$

When $\varepsilon De^2$ is equal to zero, Eq. (17) converts to a Newtonian velocity profile. The value of $\tau^*_{0l}$ is calculated through the substitution of boundary condition (16) into Eq. (17). It possesses three roots: one real and two complex roots.

$$\tau^*_{0l} = \frac{\alpha}{6\varepsilon De^2} - \frac{1}{2\alpha}(\varepsilon De^2 G^2 + 2) + \frac{1}{2}G \tag{18}$$

where

$$\alpha = \left[\left(-54 + 3\left[3\left((\varepsilon De^2)^3 G^6 + 6(\varepsilon De^2)^2 G^4 + (12G^2 + 108)(\varepsilon De^2) + 8\right)\Big/\varepsilon De^2\right]^{\frac{1}{2}}\right)(\varepsilon De^2)^2\right]^{1/3} \tag{19}$$

As a limiting case for Newtonian fluid ($\varepsilon De^2 = 0$), the first two terms of the right hand side of Eq. (18) equals $-1$ and $\tau^*_{0l}$ is equal to $\left(-1 + \frac{1}{2}G\right)$ corresponding to Newtonian dimensionless shear stress at the wall. The dimensionless distance of the velocity profile's extremum, $\kappa$, is the ratio of the dimensionless shear stress at the stationary plate ($\tau^*_{0l}$) to the dimensionless pressure gradient ($G$). At this location the shear rate is zero (Eq. (14)). The dimensionless pressure gradient is usually unknown but it is related to the cross sectional average velocity through the following equation:

$$\bar{u}^* = \int_0^1 u^* \mathrm{d}y^* \tag{20}$$

Substitution of Eq. (17) results in

$$\bar{u}^* = -\tfrac{1}{2}\tau^*_{0l} + \tfrac{1}{6}G + \varepsilon De^2\left(\tfrac{1}{10}G^3 - \tfrac{1}{2}\tau^*_{0l}G^2 + \tau^{*^2}_{0l}G - \tau^{*^3}_{0l}\right) \tag{21}$$

For Newtonian fluids, $\bar{u}^*$ equals to $\left(\frac{1}{2} - \frac{1}{12}G\right)$ (Tadmor and Gogos, 1979). The flow rate per unit width is obtained by taking the product of the average velocity and the gap between the two plates. The values of $G$ are calculated numerically using different values of the flow

rate and the viscoelastic dimensionless group. Based on the sign of the pressure gradient, $G$ may be positive or negative.

Fig. 2 presents the variation of the dimensionless average velocity as a function of the dimensionless pressure gradient ($G$) for different values of the viscoelastic dimensionless group ($\varepsilon De^2$). For negative values of the dimensionless pressure gradient, the deviation of $\bar{u}^*$ with respect to the Newtonian value increases significantly with the viscoelastic dimensionless group. This deviation increases as the dimensionless pressure gradient is decreased. For positive values of $G$, the reverse is true but the deviations are much smaller. An average velocity equal to 0.5 corresponds to a dimensionless pressure drop ($G$) of zero, which corresponds to a pure drag flow.

The shape of the velocity profile is strongly influenced by the competition between drag and pressure flow as well as by the dimensionless viscoelastic group. Fig. 3 illustrates the dimensionless velocity distributions for a value of $\varepsilon De^2$ equal to 5 and for various values of $G$. These results clearly show that the dimensionless group for pressure drop ($G$) has a major impact on the shape of the velocity profiles. Five types of dimensionless velocity distribution are obtained for a wide range of $G$ values. When $G$ is positive, the upstream pressure is lower than the downstream pressure, which may yield back flow through the channel (Fig. 3(1,2)). In this case, the direction of the pressure flow is negative while the drag flow acts in the positive direction. For negative $G$ values, the drag and pressure flows are in the same direction and positive values $\bar{u}^*$ are obtained.

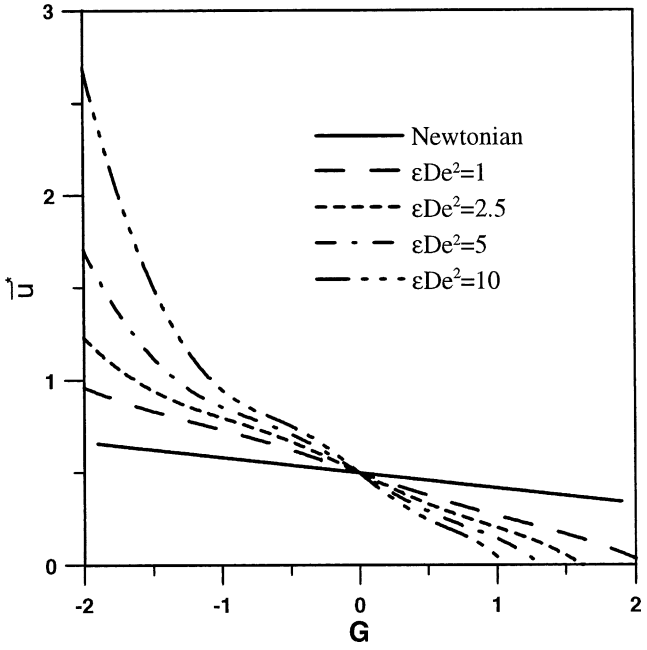


Fig. 2. The effect of the dimensionless pressure gradient on the average velocity for different viscoelastic parameters (linear stress coefficient).

The locations of the extremum of the velocity profile for different values of $\varepsilon De^2$ are shown in Fig. 4. It can be observed that there are four regions for the values of $\kappa$. Cases (a) and (b) exhibit an extremum in the velocity profile, located between the two parallel plates, corresponding to the negative and positive pressure gradients, respectively. Cases (c) and (d) are the regions where no extremum of the velocity distribution are located between the two parallel plates. Changing the elongational parameter and the Deborah number produce variations of the upper values of $G$ for case (a) and lower values for case (b) necessary to have an extremum located between the two plates. Also, the effect of $\varepsilon De^2$ is noticeable on the value of $\kappa$. Increasing the dimensionless viscoelastic group shifts downward and upward the location of the extremum for cases (a) and (b), respectively.

### 2.2. Evaluation of $f\,Re$

The fanning friction factor is defined (Shah and London, 1978):

$$f = \frac{\tau_w}{\frac{1}{2}\rho\bar{u}^2} \tag{22}$$

and

$$f\,Re = \frac{4\tau^*_{w_{ave}}}{\bar{u}^*} \tag{23}$$

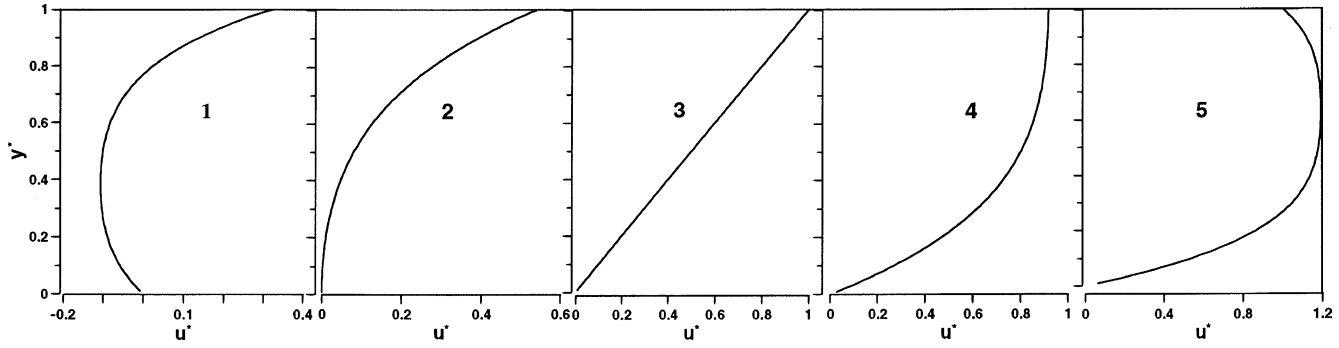


Fig. 3. Five types of velocity profile for $\varepsilon De^2 = 5$: (1) $\bar{u}^* = 0$, $G > 0$, (2) $\bar{u}^* = 0.2$, $k = 0$, $G > 0$, (3) $\bar{u}^* = 0.5$, $G = 0$, (4) $\bar{u}^* = 0.75$, $k = 1$, $G < 0$, (5) $\bar{u}^* = 1$, $G < 0$ (linear stress coefficient).

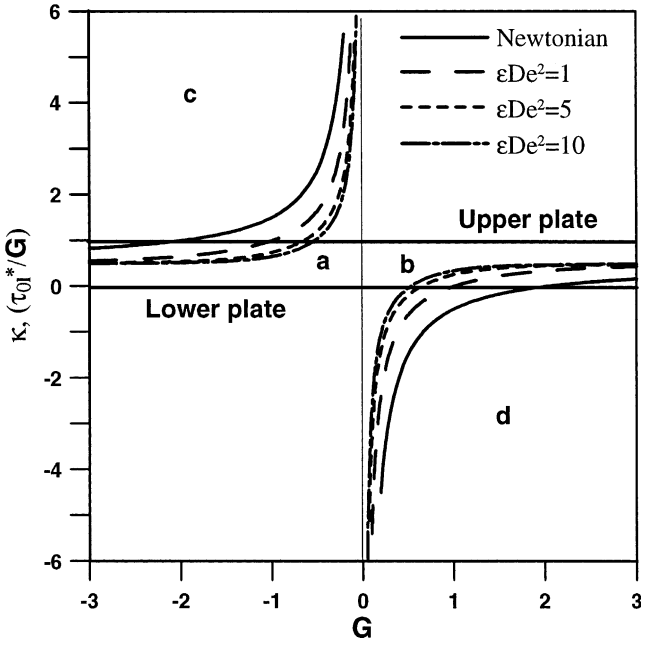


Fig. 4. The location of the velocity extremum for different dimensionless viscoelastic groups (linear stress coefficient).

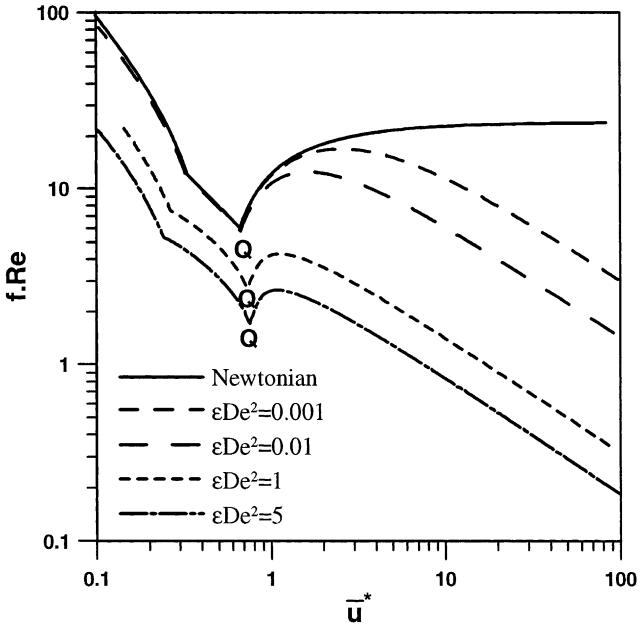


Fig. 5. The product of friction factor and Reynolds number for different dimensionless viscoelastic groups (linear stress coefficient).

where

$$\tau^*_{w_{ave}} = \frac{\tau^*_{yx}|_{y^*=0} + \tau^*_{yx}|_{y^*=1}}{2} \tag{24}$$

The dimensionless form of the shear stress can be obtained from Eq. (10):

$$\tau^*_{yx} = \tau^*_{0l} - Gy^* \tag{25}$$

For Newtonian fluids when $|G| > 2$:

$$f\,Re = \frac{24G}{G-6} \tag{26}$$

When $|G| < 2$:

$$f\,Re = \frac{48}{6-G} \tag{27}$$

From Eq. (26), when both of plates are stationary, $G$ approaches infinity and $f\,Re$ approaches 24. The variation of $f\,Re$ as a function of the average velocity is presented in Fig. 5 for fluids with different values of $\varepsilon De^2$. The value of $f\,Re$, as mentioned previously, is related to the result of the competing flow types (drag and pressure flows), and is affected by two parameters: the dimensionless wall shear stress and the average velocity (Eq. (23)). Figs. 6 and 7 show the dimensionless velocity profile and the dimensionless average wall shear stress versus the dimensionless average velocity for different values of $G$ and $\varepsilon De^2$. These figures are helpful for interpreting the behavior of $f\,Re$ as a function of $\bar{u}^*$ (Fig. 5). Within region A of Fig. 7, increasing $\bar{u}^*$ up to a certain value (point $R$) decreases the backflow (Fig. 6a and b) as well as $\tau^*_{wave}$ (Fig. 7) which yields a lower value for $f\,Re$ (Fig. 5). When the shear stress at the lower plate is zero, the value of $\bar{u}^*$ corresponds to point $R$. The velocity profile corresponding to point $R$ is the velocity profile depicted in Fig. 6b. At this point, the average velocity is equal to 1/3 for Newtonian fluid. Within region B of Fig. 7, increasing the average velocity further diminishes the backflow and the velocity gradient approaches a linear profile as depicted in Fig. 6c. The dimensionless average wall shear stress is nearly constant (Fig. 7) and $f\,Re$ decreases when $\bar{u}^*$ is increased (Fig. 5, and Eq. (23)). Point $Q$ corresponds to the situation when the wall shear stress is equal to zero at the moving plate and $G$ at lower plate. The velocity profile at point $Q$ corresponds to the profile of Fig. 6d. For $\bar{u}^* > \bar{u}^*_Q$(region C), increasing the average velocity modifies the velocity profile close to the walls (Fig. 6e and f) as well as the dimensionless average shear stress at the walls. As a result, $f\,Re$ increases.

### 2.3. Maximum pressure rise

The maximum possible pressure rise occurs when the net flow rate is zero (closed discharge condition). This condition is very important for the design of single screw extruders. Fig. 8 shows the maximum dimensionless pressure gradient ($G_{max}$) versus the dimensionless viscoelastic group ($\varepsilon De^2$). The following correlation, obtained by fitting analytical data, can be used to predict the maximum pressure drop as a function of the dimensionless viscoelastic group:

$$G_{max} = \frac{6}{[1 + 50.3(\varepsilon De^2)]^{0.273}} \tag{28}$$

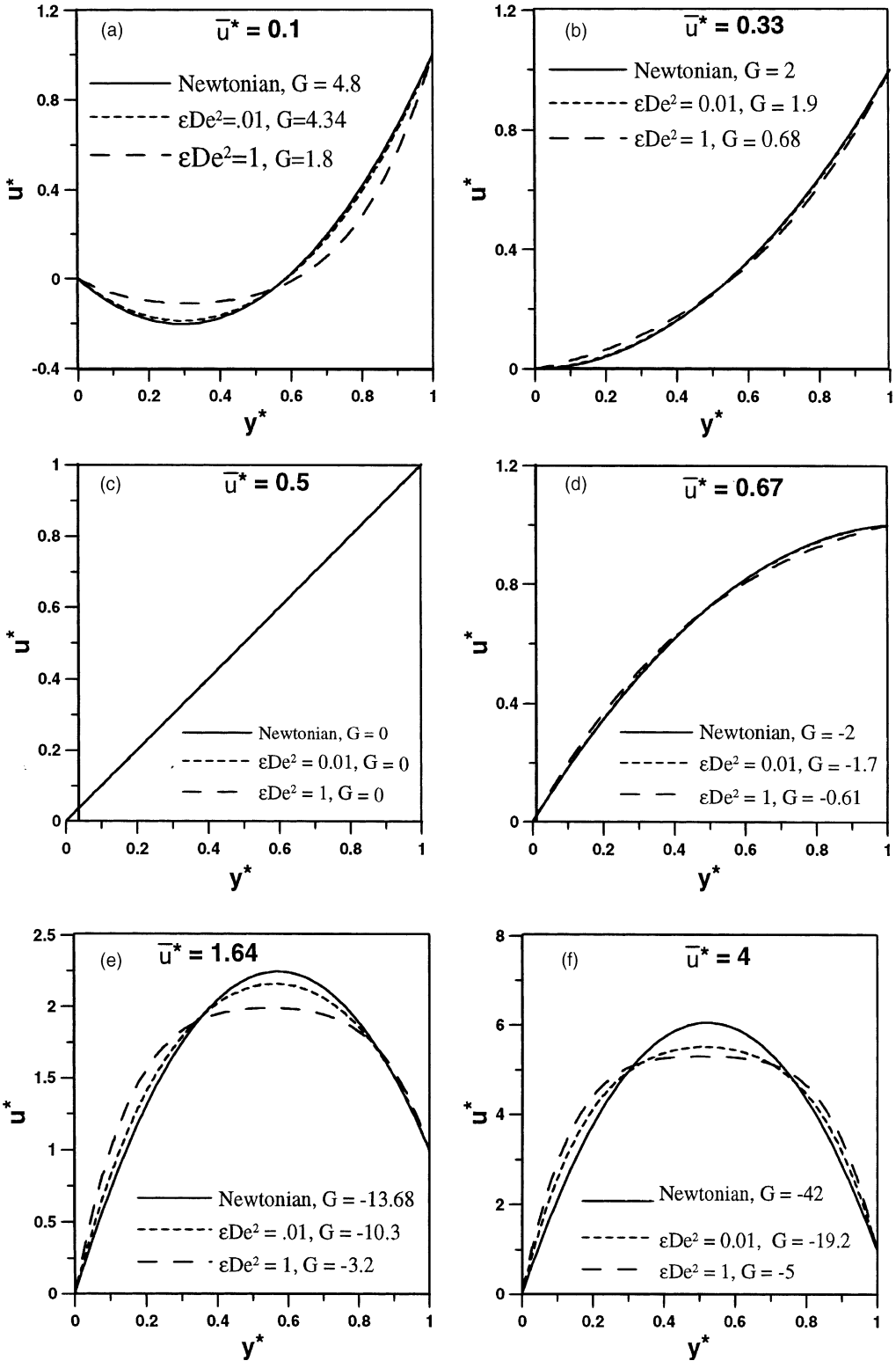


Fig. 6. Dimensionless velocity profile for different values of $\bar{u}^*$, $G$ and $\varepsilon De^2$ (linear stress coefficient).

This correlation is an accurate representation of the maximum pressure drop variation. In addition, this correlation is also valid for Newtonian fluids as it reduces to a $G_{\max}$ value of 6 (Tadmor and Gogos, 1979). The total dimensional pressure rise is:

$$\Delta p_{\max} = \frac{6}{[1 + 50.3(\varepsilon De^2)]^{0.273}} \frac{\eta V L}{H^2} \tag{29}$$

where $L$ is the length of the plates. Small values of $\varepsilon De^2$ correspond to Newtonian fluids and the maximum di-

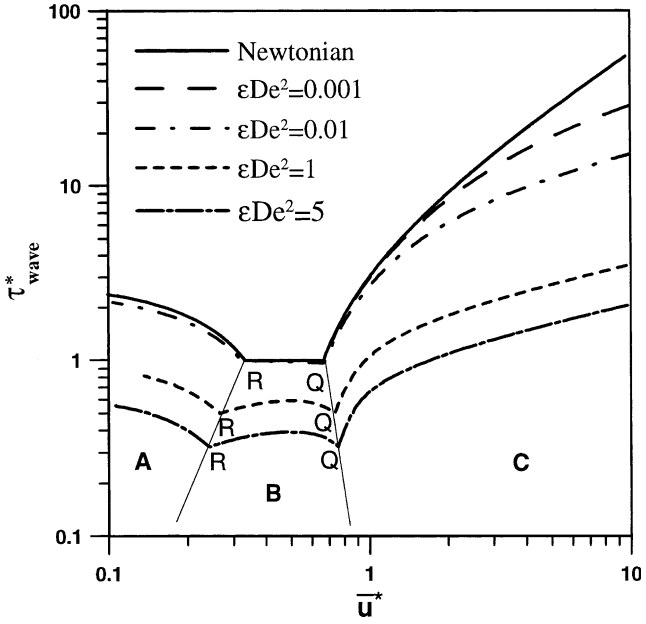


Fig. 7. The variation of the dimensionless average shear stress with the dimensionless average velocity for different values of $\varepsilon De^2$ (linear stress coefficient).

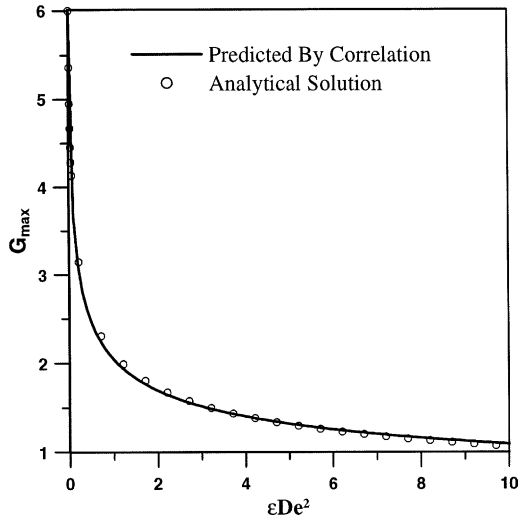


Fig. 8. The maximum pressure rise as a function of the dimensionless viscoelastic group.

mensionless pressure drop approaches a value of 6. The maximum pressure rise for viscoelastic fluids is that for Newtonian fluids with a correction factor of $1/([1+50.3(\varepsilon De^2)]^{0.273})$.

### 2.4. Exponential stress coefficient

The linear form of the stress coefficient leads to valid results for small liquid deformations. The exponential

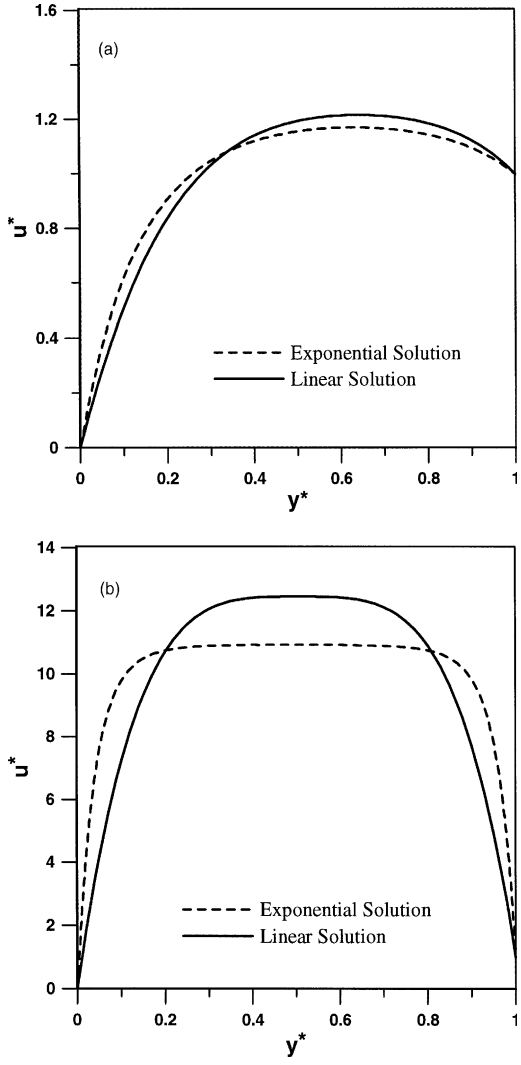


Fig. 9. Comparison of dimensionless velocity profile: (a) $\bar{u}^* = 1$, $\varepsilon De^2 = 1$ and (b) $\bar{u}^* = 10$, $\varepsilon De^2 = 10$.

form of the stress coefficient should be used for strong flow (Tanner, 2000). Substitution of the exponential coefficient and the solution of the counterpart equations of the linear profile give the following equation:

$$u^* = \frac{1}{4\varepsilon De^2 G}\left[\exp(2\varepsilon De^2(\tau_{0e}^* - Gy^*)^2) - \exp(2\varepsilon De^2 \tau_{0e}^{*2})\right] \tag{30}$$

$G$ and $\tau_{0e}^*$ are calculated through the system of non-linear equations (20) and (30), using the moving plate boundary conditions.

Fig. 9a and b present the comparison of the dimensionless velocity profile for both linear and exponential stress coefficients for different values of the average velocity and of the dimensionless viscoelastic group. These results show that using the exponential form of stress coefficient results in a flatter dimensionless velocity distribution. The difference between the

two cases is more pronounced for higher values of $\bar{u}^*$ and/or $\varepsilon De^2$.

## 3. Conclusions

An analytical solution was obtained for steady laminar, incompressible flow of SPTT model fluid through parallel plates when the upper plate is moving at constant speed whereas the lower plate is stationary. Two different forms of stress coefficient were employed. Results for the linear stress coefficient emphasize the appreciable influence that $\varepsilon De^2$ has on the flow behavior of viscoelastic fluids. When $G < 0$, an increase in the viscoelastic dimensionless group leads to an increase in the dimensionless average velocity for a combined drag and pressure flow, whereas the reverse behavior occurs when $G > 0$. Five types of velocity distribution were obtained based on the combined effects of pressure and drag flows. In addition, the influence of $\varepsilon De^2$ on $f Re$ is noticeable. Increasing $\varepsilon De^2$ diminishes the value of the product of the friction factor and the Reynolds number.

The pressure rise is controlled by manipulating the opening of the valve far from the inlet of the extruder and when the valve is fully closed the pressure is maximum. In this investigation, an accurate correlation for the maximum pressure rise as a function of the dimensionless viscoelastic group was obtained.

If the exponential stress coefficient is used, the velocity profile is nearly identical to the profile obtained with the linear stress coefficient for low values of $\varepsilon De^2$ and/or the flow rate, whereas for high values of these parameters significant deviations are observed.

## References

Alves, M.A., Pinho, F.T., Oliveira, P.J., 2001. Study of steady pipe and channel flows of single-mode Phan-Thien–Tanner fluid. J. Non-Newtonian Fluid Mech. 101, 55–76.

Bird, R.B., Amstrong, R.C., Hassager, O., 1978. Dynamics of Polymeric Liquids, Fluid Mechanics, vol. 1, second ed. John Wiley, New York.

Davaa, G., Shigeehi, T., Momoki, S., Jambal, O., 2001. Fluid flow and heat transfer to modified power law fluids in plane Couette-Poiseuille laminar flow between parallel plates. Reports of the Faculty Engineering, Nagasaki University, vol. 31, no. 57, pp. 31–40.

Gopalakrishna, S., Jaluria, Y., 1992. Heat and mass transfer in single screw extruder for non-Newtonian material. Int. J. Heat Mass Transf. 35 (1), 221–237.

Oliveira, P.J., Pinho, F.T., 1999. Analytical solution for fully developed channel and pipe flow of Phan-Thien–Tanner fluids. J. Fluid Mech. 387, 271–280.

Phan-Thien, N., Tanner, R.I., 1977. A new constitutive equation derived from network theory. J. Non-Newtonian Fluid Mech. 2, 353–365.

Phan-Thien, N., 1978. A nonlinear network viscoelastic model. J. Rheo. 22, 259–283.

Pinho, F.T., Oliveira, P.J., 2000. Analysis of forced convection in pipes and channels with the simplified Phan-Thien Tanner fluid. Int. J. Heat Mass Transf. 43, 2273–2287.

Shah, R.K., London, A.L., 1978. Laminar Flow Forced Convection in Ducts. Academic Press, Inc, New York.

Tadmor, Z., Gogos, C., 1979. Principles of Polymer Processing. John Wiley and Sons, New York.

Tanner, R.I., 2000. Engineering Rheology. Clarendon Press, Oxford.